Detonation Front Structure: Variety and Characterization

F. Pintgen, J.M. Austin, and J.E. Shepherd
Graduate Aeronautical Laboratories,
California Institute of Technology
Pasadena, California 91125

Abstract

The structure of multifront or cellular detonation waves has been studied using Schlieren, planar laser-induced fluorescence (PLIF) imaging of the OH radical, and soot foils in three mixtures with varying regularity. These are: stoichiometric H_2-O_2 diluted with Ar, stoichiometric H_2-O_2 diluted with N_2, and stoichiometric H_2-N_2O diluted with N_2, all at 20 kPa initial pressure. Very different structures are observed in each mixture. These differences are most striking on the PLIF images, which are used as a starting point for a qualitative discussion and interpretation of the features seen on the Schlieren images and soot foils. It is clear that the propagation mechanism of mixtures with irregular cellular structure may be much more complex than for mixtures with regular cellular structure.

Introduction

Many researchers have investigated the structure of propagating detonation waves experimentally and more recently, through numerical simulation. The initial evidence of the multifront or "cellular" structure of detonation waves was obtained by White (1961) with interferometry, Denisov and Troshin (1959) using foils covered with a thin layer of soot, and Schlieren methods by Soloukhin (1965). The interferometric measurements demonstrated the existence of secondary transverse waves propagating nearly perpendicular to the front and a curved front structure with abrupt changes in slope at triple points where the secondary waves joined the main front. The modern view of the structure of multifront detonations was initiated with the pioneering work of Voitsekhovskii et al. (1963).

The simple technique of soot foils has been used extensively to investigate the shock configurations of the front and in particular to study the wave configurations at the triple points. Lee et al. (1969) made stroboscopic Schlieren photographs through a sooted window to show the tracks are closely associated with the triple points on the detonation front, although the physical mechanism by which the tracks are made in the soot layer is still unclear. Soot-foil track angles may be used to calculate triple-point configurations using shock polars once the angle of the track and the velocity of the leading shock through the cell is known (Strehlow et al., 1967, Oppenheim et al., 1968, Urtiew, 1970, Subbotin, 1975). These techniques and numerical simulation were used recently by Pintgen et al. (2003) to calculate OH contours at the triple point for comparison with PLIF images.

Soot foils have also been previously used to characterize the cellular regularity of detonation structure. Strehlow (1969) and Libouton et al. (1981) classified many mixtures in this manner and observed that highly Ar-diluted mixtures have a very regular structure while N_2 diluted mixtures have a more irregular structure. In C_2H_2-N_2O-Ar mixtures, Libouton et al. (1981) also observed "substructure" – cellular soot foil tracks similar in appearance to the large scale structure but appearing at multiple scales smaller than the main cell size. The substructure cells are observed on the soot tracks in the upstream apex of the main cell and increase in size as the velocity of the Mach stem decays. They are usually not observed in the second half of the main cell.

Schlieren and interferometry have previously been used to visualize shock and reaction zone structure in detonation waves. Because of the difficulties associated with interpreting these images in three-dimensions, many studies have been performed in narrow channels (Voitsekhovskii et al., 1963, Edwards et al., 1972, Strehlow and Crooker, 1974). Subbotin (1975) reported different triple point structures in different mixtures. Using Schlieren images, Subbotin calculated that the transverse waves were unreactive in irregular (CH_4-O_2) mixtures and reactive in a regular (H_2-O_2-Ar) mixture. Subbotin also reported islands of unburnt gas that become isolated from the main front after a triple point collision. Such "unburnt pockets" were also observed in Schlieren images by Edwards (Oran et al. 1982).

Previous researchers have made substantial progress in describing the structure of multi-front (cellular structure) detonation waves. One of the key issues that remains unresolved is the precise nature of the combustion processes within the reaction zone. To make progress on this issue, it is necessary to use techniques that are sensitive to chemical species and spatially resolve the structure in the front. For detonation front studies on irregular mixtures in wide channels, integrating techniques such as direct imaging of chemiluminescence appear to be limited in value. Much more promising are techniques such as PLIF that allow the dissection of the flow into planar sections.

Andresen et al. (1992) used laser induced predissociation fluorescence (LIPF) to obtain images of oscillations along the reaction zone front of detonation waves, Eder (2001) made LIPF images of fast deflagrations, and Pintgen (2000) used OH PLIF to image the cellular character of the reaction zone structure of detonations. Very striking features with a "keystone" shape were observed by Pintgen (2000) in many mixtures and we demonstrated previously (Pintgen et al., 2003) that these features can be interpreted in terms of classical shock-induced combustion for mixtures highly diluted with argon. The appearance of these features can be related to the oscillations in shock front strength and the substantial changes in the OH concentration across the shear layer associated with the triple-points. The keystone features appeared more irregular for the N_2-diluted mixtures than for the Ar-diluted mixtures. The present study is an extension of the authors' previous work and focuses on differences observed in mixtures with various degrees of regularity.

Experimental Technique

The experiments were carried out in a 280 mm diameter detonation tube coupled by a 150 mm square "cookie-cutter" to a 150 mm square test section. The overall length of the facility is 8 m; the length of the cookie-cutter and test section is 1.5 m. The tube is evacuated to approximately 0.04 kPa before each filling procedure, which is based on the partial pressure of each species. The detonation is initiated directly by a thin copper wire exploding in a small amount (10% of the tube volume) of acetylene-oxygen mixture , which is injected into the tube immediately prior to ignition. Pressure traces and detonation velocities are obtained from six pressure transducers located along the facility, three of which are in the test section. Soot foils were placed on the sidewalls of the test section as well as on the end plate of the test-section.

Simultaneous Schlieren and OH PLIF visualizations are made through two 184 mm diameter windows in the side walls of the test section. The light source for the Schlieren system is a Q-switched ruby laser with a 50 ns pulse width. The Schlieren system is a typical Z-setup using two concave mirrors of focal length 1 m. The transmitted light passes through a narrow bandpass filter to eliminate self-light from the detonation and is imaged onto 80×100 mm black and white Polaroid (3000 ISO) film. The laser system for the PLIF setup consists of a tuneable dye laser (Scanmate2E, Lambda Physik) with a frequency doubling unit which is pumped by an excimer-laser (COMPex102, Lambda Physik). The pulse energy of the excimer laser is 300 mJ and the pulse width approximately 17 ns. A Coumarin 153 dye was used in the dye-laser to obtain a narrow band UV light with a pulse energy of about 6.5 mJ. The frequency was tuned to 284.008 nm which corresponds to the immediate vicinity of two OH-transitions: $A^2\Sigma^+ \leftarrow X^2\Pi_i(1,0)$ $Q_2(8)$ and $A^2\Sigma^+ \leftarrow X^2\Pi_i(1,0)$ $Q_1(9)$.

The UV laser beam is directed by mirrors to propagate along the tube axis and formed into a light sheet by a combination of a cylindrical lens (focal length -25 mm) and a spherical lens (focal length 1000 mm). The light sheet enters the test section through a quartz window in the center of the test section end plate. The induced fluorescence is perpendicular to the light sheet, passes through a 184 mm diameter quartz glass window, and is filtered by a bandpass filter (centerline 313 nm, FWHM 10 nm) before being imaged by a 576×384 pixel 12 bit intensified CCD-Camera (Princeton Instruments ITE/ICCD-576). The image is formed by a 105 mm f/4.5 UV-transmitting lens (Nikkon UV-Nikkor). The camera was gated by a 90 ns pulse of 900 V. Depending on the height of the field of view of the camera, which was varied between 80 and 30 mm, the light sheet-forming optics were readjusted such that the usable light sheet height was optimized. For simultaneous Schlieren and PLIF experiments, the camera had to be placed out of the optical path of the Schlieren setup and therefore at a slight angle (under 15°) to the desired perpendicular position relative to the light sheet. The resulting distortion was corrected by postprocessing the PLIF image using a test-pattern to match images obtained from both systems.

Two photo diodes detecting the light pulse emitted from the ruby laser and the dye-laser verified that the time between acquiring the Schlieren image and the PLIF image

was less than 200 ns. The current investigation is qualitative rather than quantitative due to the non uniformity of the light sheet and locally varying effects influencing the fluorescence intensity. These effects include varying excited state population which depends on the local thermodynamic state and molecular effects like quenching which is influenced by the number density of the quenching species. Three-dimensional effects due to the orientation of the cellular structure to the light sheet are evident on the end plate soot foils.

Results

This work is part of a larger program in detonation research which has as one goal the understanding of the combustion mechanisms and dynamics of detonation fronts. To this end, experiments were carried out with several different mixtures, all using hydrogen as the fuel. Stoichiometric H_2-O_2-Ar, H_2-O_2-N_2, and H_2-N_2O-N_2 mixtures were investigated. The H_2-O_2-Ar mixture represents a mixture with a very regular cellular structure. The N_2-diluted H_2-O_2 mixture is an example of an irregular cellular structure, whereas the H_2-N_2O mixture diluted with N_2 has a highly irregular cellular structure. Previously, cellular substructure has been observed in the H_2-N_2O system (Libouton et al., 1981). All experiments were conducted at an initial temperature of 25°C and an initial pressure of 20 kPa. One PLIF and one Schlieren image is obtained from each experiment. Schlieren images, pressure histories, and soot foil records indicate the detonations are multi-front, self-sustaining waves within the test section. We have obtained many images in the course of our experiments and only show a few examples here.

Ar-diluted H_2-O_2 mixtures

The detonation velocities were within 1.5% of the Chapman-Jouguet value for the 80% and 85% Ar-diluted H_2-O_2 mixture in the round cross-section of the facility. The soot foils placed in the test section confirmed the expected high regularity of this mixture (Fig. 1a). The cell size for the 80% Ar-diluted case was measured to be 22 mm and 48 mm which is 7 and 3 times less respectively the test section dimension. The regularity is seen in the relatively small variations in the cell size. End plate soot foils show that the two planes of the detonation are not repeatably orthogonally aligned to the side walls for every experiment. The orthogonal structure appears to be most often observed for the 80% diluted mixture.

Transverse waves extending into the unburned region can be identified on the Schlieren images. The visibility of the transverse waves depends in large part on the alignment of the waves relative to the optical axis. The transverse waves are most clearly visible when the waves are propagating in two orthogonal families that are parallel to the test section walls. In these cases, as shown in Fig. 1b, the flow field behind the main front appears to be composed of periodic transverse shock waves with a spacing on the order of the cell size. The leading shock wave is imaged as a sharp line with a smooth contour. There do not appear to be any significant small-scale features visible in the Schlieren images.

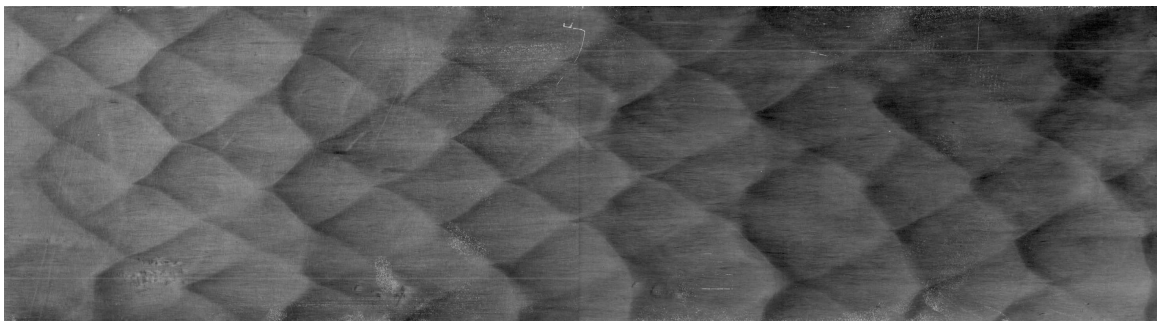

a) Shot 1649

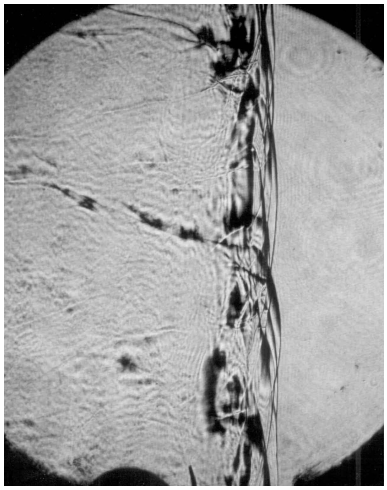

b) Shot 1688

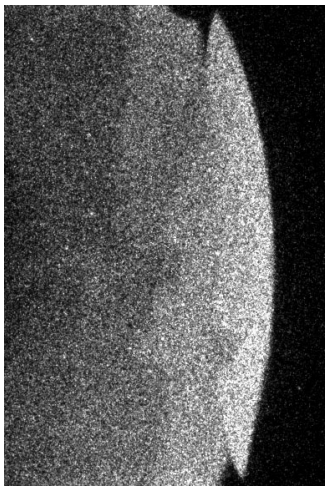

c) Shot 1676

Figure 1: a) Side wall soot foil (image height 150 mm) of 85% Ar-diluted stoichiometric H_2-O_2 mixture. b) Schlieren image of detonation front (image height 150 mm) and c) PLIF image of OH fluorescence behind the detonation front (image height 30 mm) in a stoichiometric H_2-O_2 mixture diluted with 87% Ar. The initial pressure is 20 kPa for all mixtures and the detonation wave propagates from left to right in all images.

In PLIF images (Fig. 1c) for these Ar-diluted mixtures, a distinct front is seen which corresponds to the sharp increase in OH concentration at the end of the induction zone. The PLIF images reveal a very smooth reaction front punctuated periodically with the previously reported (Pintgen et al. 2003) "keystone" features associated with the oscillation of the detonation front velocity. The keystone is bounded by a discontinuity in reactivity across the shear layers that emanate from the triple points at the intersection of the transverse waves and main front. This can be most clearly seen in Fig. 2, which shows an overlay of the Schlieren and PLIF images. The PLIF image is a close up and the straight edges on top, bottom, and left are associated with the PLIF-image boundaries. Near the top of the image, a transverse wave can clearly be seen and associated with the triple point shown in the Schlieren image.

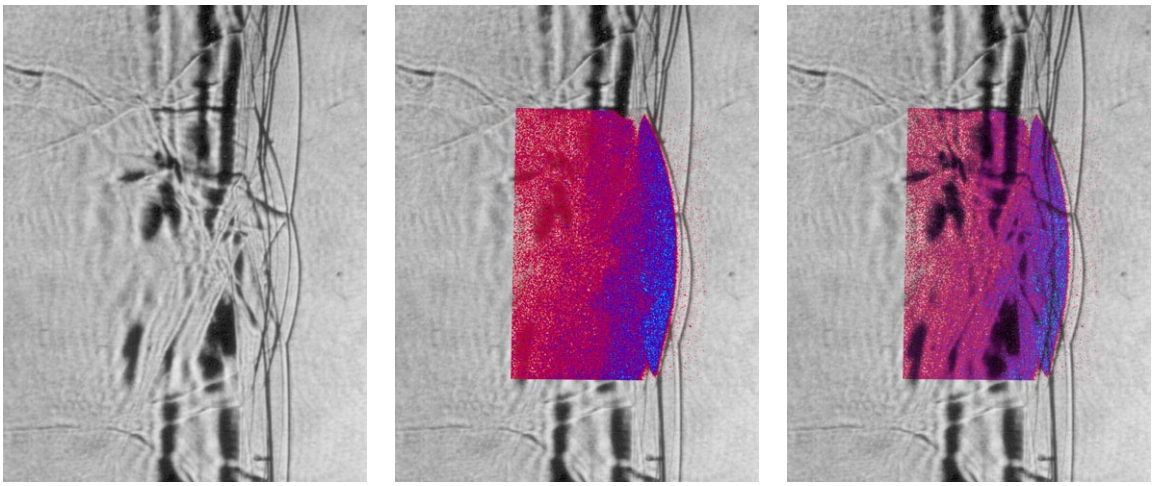

a) Shot 1676 b) Shot 1676 c) Shot 1676

Figure 2: 87% Ar-diluted stoichiometric H_2-O_2 mixture, Shot 1676. a) Schlieren image . b) Superposure of false color PLIF image with Schlieren image. c) Overlay of PLIF and Schlieren image. Schlieren image is 50 mm high and PLIF image is 30 mm high.

The role of the transverse waves is not completely resolved but in many of Ar-diluted cases we have examined, they do not appear to play a essential role in the combustion (Fig. 1b, c). The "keystone" is less pronounced in a some cases and may depend on the stage in the cell cycle when the image is captured. Other than three-dimensional effects associated with the misalignment of the transverse waves with respect to the light sheet, the OH distribution appears to be contiguous. The reaction front is slightly curved behind the incident shock and the Mach stem. The discontinuity across the shear layer appears as a smooth straight line at the highest resolution (20 pixel/mm) used in these experiments.

N_2-diluted H_2-O_2 mixtures

For the N_2-diluted H_2-O_2 mixtures, the soot foils (Fig. 3a) indicate a wider range of cell sizes and track angles compared to the Ar-diluted mixtures with comparable cell size. The cell size for 45% N_2 and 65% N_2 was measured to be 22 mm and 55 mm respectively. The wave system at the front rarely appears to be to be aligned in an orthogonal fashion to the test section walls and coherent transverse wave structures are not visible on the Schlieren images (Fig. 3b) or end plate soot foils (not shown). On the Schlieren images, the leading shock wave appears to be much less planar than for the Ar-diluted mixture with the same cell size. The curved sections visible along the front do not correspond to the cell size measured on the soot foils. In part, this may also be due to the integrating effect of the Schlieren image and the lack of coherence in the transverse wave structures. Behind the shock front, small-scale variations in density gradients are visible at a distance up to one cell size downstream of the leading shock. The PLIF images show that the

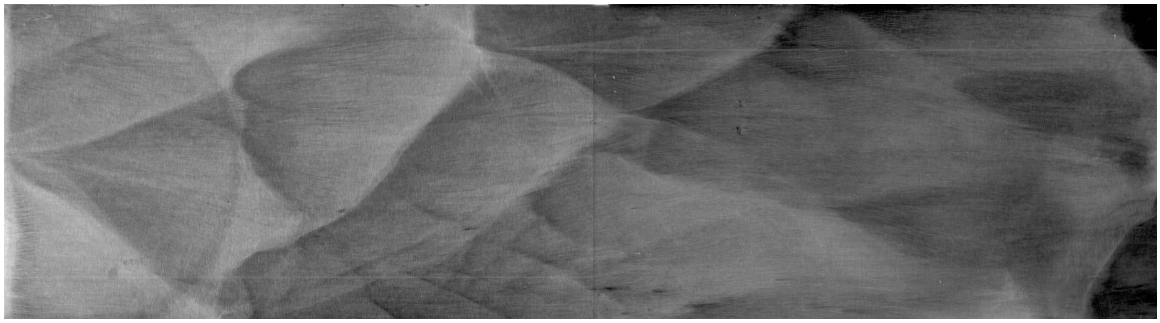

a) Shot 1673

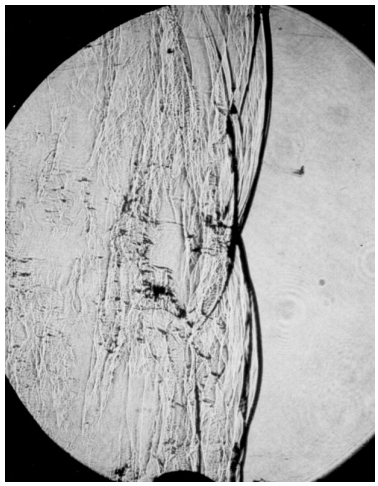

b) Shot 1605

c) Shot 1604

Figure 3: a) Side wall soot foil (image height 150 mm), b) Schlieren image of detonation front (image height 150 mm), and c) PLIF image of OH fluorescence behind the detonation front (image height 50 mm) in a stoichiometric H_2-O_2 mixture diluted with 72% N_2 . The initial pressure is 20 kPa for all mixtures and the detonation wave propagates from left to right in all images.

reaction front is much more distorted (Fig. 3c and 4) than in the Ar-diluted cases. For cell sizes up to 55 mm and resolutions up to 10 pixel/mm, the "keystone" features associated with the cellular structure are still seen, but the front separating regions of high and low fluorescence are in general much more wrinkled. Disturbances in the OH front are visible on scales less then the cell size determined from soot foil measurements. For higher resolution (20 pixel/mm) imaging and higher N_2 dilution (72.7%) cases, features are visible which resemble those commonly associated with Kelvin-Helmholtz instability for shear layers.

These features were not observed in the case of Ar-diluted mixtures with similar velocity differences and only sometimes observed in N_2-diluted mixtures. We speculate that lack of consistent observation of shear-layer instabilities is related to the resolution

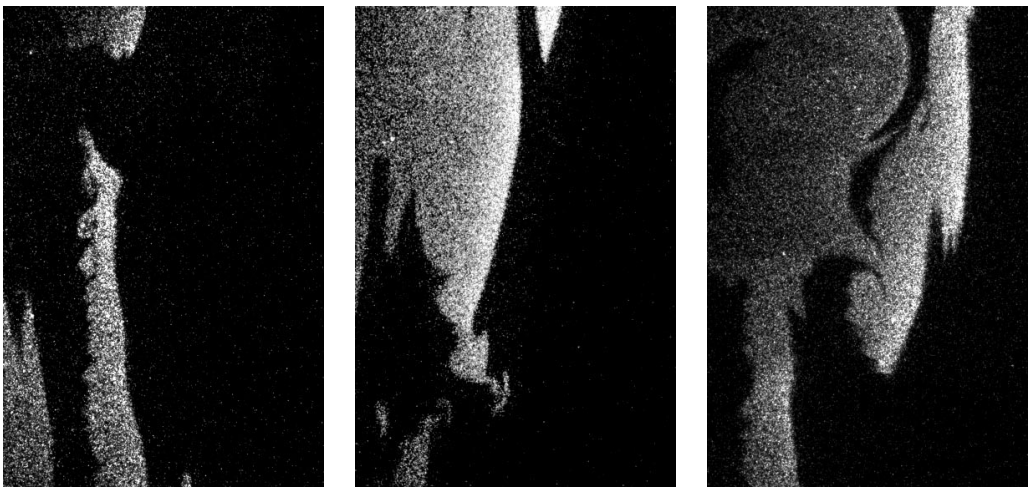

a) 72% N_2 Shot 1598 b) 75% N_2 Shot 1633 c) 75% N_2 Shot 1635

Figure 4: Selection of PLIF images of OH fluorescence behind the detonation front in a stoichiometric H_2-O_2 mixture diluted with N_2. The initial pressure is 20 kPa and the detonation wave propagates from left to right in all images. Image height: a) 30mm, b) and c) 50mm

of the images and the size of the cells in comparison to the test section dimensions. A possible explanation for the differences in Ar and N_2-diluted mixtures is the difference in extent of the OH concentration gradient across the shear layer in the two cases, see the discussion below. Further investigation is required to resolve this issue. The complex nature of the flow field suggests that simultaneous planar imaging of the shock front and OH front will required to make progress on this aspect.

H_2-N_2O-N_2 mixtures

For the H_2-N_2O-N_2 mixtures, 50% and 60% N_2 diluted mixtures were investigated and cell sizes of 42 mm and 70 mm measured on the soot foils. In both cases, substructure was seen on the side wall soot foils (Fig. 5a). The structure originates at the upstream end (apex) of the cells and persists until the middle of the cell. The size of the substructure cells increases with increasing distance downstream from the cell apex. The end plate soot foils (not shown) also showed the highly irregular structure seen on the side wall soot foils. The Schlieren images (Fig. 5b) reveal that the leading shock front is strikingly different than the previous cases studied. In addition to the smooth curved waves observed with Ar and N_2-diluted mixtures, we can observe "rough" portions with fine scale disturbances on the front. The region immediately behind the main shock front contains fine-scale density fluctuations that persist for a distance of about one cell size behind the front. The large scale cellular structure as seen in the other two mixtures is not as striking for the 60% N_2O-diluted mixture and vanishes nearly entirely for the 50%-diluted case on the Schlieren images. The transverse waves are difficult to discern due to the presence

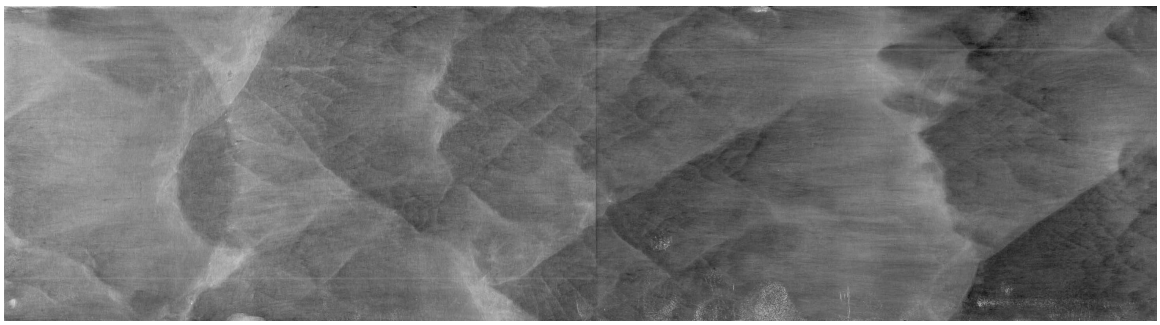

a) Shot 1642

b) Shot 1609

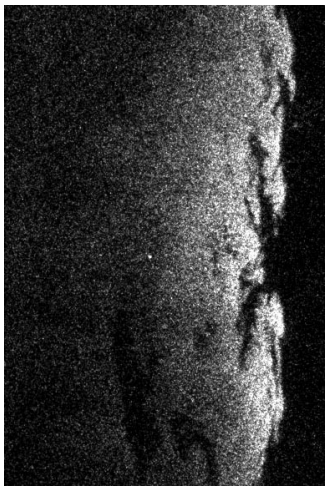

c) Shot 1607

Figure 5: a) Side wall soot foil (image height 150 mm), b) Schlieren image of detonation front (image height 150 mm), and c) PLIF image of OH fluorescence behind the detonation front (image height 45 mm) in a H_2-N_2O-$3N_2$ mixture. The initial pressure is 20 kPa.

of small-scale density disturbances. The complexity of the flow makes relating Schlieren images to PLIF images even more difficult than in the N_2 diluted case.

The PLIF image (Fig. 5c) is clearly different from either the Ar or N_2-diluted cases. The "keystone" features are not as distinct and the OH front is very rough rather than smooth. Instead of a contiguous front, there appear to be isolated irregular regions of low intensity embedded within the high intensity region behind the main OH front.

Discussion

Several new features have been observed in the present experiments that were not seen in our previous studies (Pintgen 2000 and Pintgen et al. 2003). The most significant are a) shear-layer type disturbances on the OH front in N_2-diluted mixtures and b) fine scale

density and OH front disturbances in H_2-N_2O-N_2 mixtures.

The presence of features commonly associated with shear-layer instabilities is hardly surprising given the large velocity differences that three-shock models (Pintgen et al. 2003) predict across the contact surface between the flow behind the Mach stem and the reflected wave. Visual evidence of turbulent shear layers was seen in earlier Schlieren images (see p. 76, shot 136 of Akbar 1997) obtained in our laboratory in a stoichiometric H_2-O_2 mixture with 88% Ar dilution. What is somewhat surprising is that these features are not also observed on the PLIF OH front images in 87% Ar-diluted mixtures but are visible in the 72.7% N_2-diluted mixture. We speculate that the difference in visibility by the OH PLIF technique is due to the difference in OH concentration across the shear layers in these two cases: Apparently in the N_2-diluted cases, a large OH concentration difference occurs across a substantial extent of the shear layer while in the Ar-diluted cases the OH concentration is only appreciably different very close to the triple point. Evidence of shear layer instability for the highly N_2 diluted mixtures is very faint on the Schlieren images. We believe that this is due to the rather modest density gradients in the shear layers as compared to the shock waves, lack of alignment of the shear layers with respect to the optical path, and the obscuring effects of the small-scale density fluctuations distributed randomly behind the leading shock front.

The appearance of the OH PLIF images for the H_2-N_2O mixtures is intriguing. On the basis of our previous work with Ar-diluted mixtures, we anticipated that the substructure visible on the soot foils might be manifested as a superposition of "keystone" features of varying sizes. Instead, it is difficult to recognize distinct keystones in the OH PLIF images and transverse waves that would be associated with the substructure are difficult to observe on the Schlieren images. With the current resolution, the ordered features seen for the Ar-diluted mixtures are not seen on any scale. The fine-scale structure in the Schlieren images taken together with the fine-scale wrinkling of the OH fronts suggests that velocity and density fluctuations on a scale much smaller than the main cell width are important issues in mixtures with highly irregular cellular structure.

Conclusions

Several experimental techniques were used to investigate different properties of the flow field behind propagating detonation waves. Three mixtures were chosen as representative of regular, irregular and very irregular cellular structure. In Ar-diluted H_2-O_2 mixtures with regular structure, soot foils show a very regular pattern, Schlieren images show disturbances to the main front in the order of the cell size and "keystone" features are seen in the PLIF images. In more irregular N_2-diluted H_2-O_2 mixtures, soot foils show a wider range of cell sizes, and Schlieren images show structures with a scale smaller than the cell width. Highly N_2-diluted mixtures exhibit features on the PLIF images which suggest the instability of the shear-layer. In very irregular N_2O-H_2-N_2 mixtures, features with a size much smaller than the main cell width appear, soot foils show substructure, a finely subdivided, more unstructured flow field is visible on the Schlieren images, and very convoluted OH fronts are observed in the PLIF images. From the photographic evidence,

it appears that shear flow instabilities and fine-scale wrinkling of the OH front may play a role in the combustion mechanism of mixtures with irregular cellular structure. Continued experimentation and improved diagnostics are needed to fully resolve the nature of the combustion processes within the detonation front in the case of mixtures with highly irregular cellular structure.

Acknowledgements

This work was supported by the Office of Naval Research, Multidisciplinary University Research Initiative *Multidisciplinary Study of Pulse Detonation Engine*, grant 00014-99-1-0744, subcontract 1686-ONR-0744.

References

Akbar, R. (1997, August). *Mach Reflection of Gaseous Detonations*. Ph. D. thesis, Rensselaer Polytechnic Institute, Troy, New York.

Andresen, P., W. Reckers, H. Wagner, E. Dabora, and H. Voges (1992). The structure of gaseous detonations as revealed by laser-induced fluorescence of the oh-radical. *Zeitschrift fur Physicalische Chemie Neue Folge 175*, 129–143.

Denisov, Y. and Y. Troshin (1959). Pulsating and spinning detonation of gaseous mixtures in tubes. *Dokl. Akad. Nauk. 125*, 110–113.

Eder, A. (2001, January). *Brennerverhalten schnallnaher und überschall-schneller Wasserstoff-Luft Flammen*. Ph. D. thesis, Technische Universität München, Munich, Germany.

Edwards, D., G. Hooper, and R. Meddins (1972). Instabilities in the reaction zones of detonation waves. *Astronautica Acta 17*(4-5), 475–485.

Lee, J., R. Soloukhin, and A. Oppenheim (1969). Current views on gaseous detonation. *Astronautica Acta 14*, 565–584.

Libouton, J., A. Jacques, and P. Van Tiggelen (1981). Cinétique, structure et entretien des ondes de détonation. *Actes du Colloque International Berthelot-Vieille-Mallard-Le Chatelier 2*, 437–442. Bordeaux.

Oppenheim, A., J. Smolen, and L. Zajac (1968). Vector polar method for the analysis of wave intersections. *Combust. Flame 12*, 63–76.

Oran, E., T. Young, J. Boris, J. Picone, and D. Edwards (1982). A study of detonation structure: The formation of unreacted gas pockets. In *19th Symposium (International) on Combustion*, Pittsburgh, PA, pp. 573–582. The Combustion Institute.

Pintgen, F. (2000, December). *Laser-Optical Visualization of Detonation Structures*. Diplomarbeit, Lehrstuhl für Thermodynamik: Technische Universität München / Graduate Aeronautical Laboratories: California Institute of Technology, Munich, Germany.

Pintgen, F., C.A.Eckett, J.M.Austin, and J.E.Shepherd (2003). Direct observations of reaction zone structure in propagating detonations. *Combust. Flame (in press)*.

Soloukhin, R. (1965). Multiheaded structure of gaseous detonation. *Combust. Flame 9*, 51–58.

Strehlow, R. (1969). The nature of transverse waves in detonations. *Astronautica Acta 14*, 539–548.

Strehlow, R. and A. Crooker (1974). The structure of marginal detonation waves. *Acta Astronautica 1*, 303–315.

Strehlow, R., R. Liaugminas, R. Watson, and J. Eyman (1967). Transverse wave structure in detonations. In *11th Symposium (International) on Combustion*, Pittsburgh, PA, pp. 683–692. The Combustion Institute.

Subbotin, V. (1975). Two kinds of transverse wave structures in multi-front detonation. *Fizika Goreniya i Vzryva 11*(1), 96–102.

Urtiew, P. (1970). Reflections of wave intersections in marginal detonations. *Astronautica Acta 15*, 335–343.

Voitsekhovskii, B., V. Mitrofanov, and M. Topchian (1963). Struktura fronta detonastii i gaza. *Akad. Nauk., SSSR, Novosibirsk*. Translation: The structure of a detonation front in gases Rep. FTD-MT-64-527, Foreign Technology Division, Wright-Patterson A.F.B., Ohio,(1966).

White, D. (1961). Turbulent structure in gaseous detonations. *Phys. Fluids 4*, 465–480.